Journal of Metals, Materials and Minerals, Vol. 30, No. 3, pp. 30-37, 2020

Optical properties of TiO_2@Ag nanowires and nanospheres

Thananchai DASRI[1,*], Panuwat CHAIYACHATE[2], Sasiporn AUDTARAT[1], Panadda CHAREE[1], and Artit CHINGSUNGNOEN[3]

[1] *Faculty of Interdisciplinary Studies, Khon Kaen University, Nong Khai Campus, Nong Khai, 43000, Thailand*
[2] *School of Science and Mathematics, Faculty of Industrial and Technology, Rajamangala University of Technology Isan Sakon Nakhon Campus, Sakon Nakhon, 47160, Thailand*
[3] *Technological Plasma Research Unit, Department of Physics, Faculty of Science, Mahasarakham University, 44150, Thailand*

[*]**Corresponding author e-mail:** thananchai_dasri@hotmail.com

Received date:
8 November 2019
Revised date:
11 June 2020
Accepted date:
16 June 2020

Keywords:
TiO_2@Ag core-shell nanostructure
Absorption property
Localized surface plasmon resonance

Abstract

Nanoparticles (NPs) with nonmetallic cores and metallic shells (such as Au, Ag, and Cu) can exhibit improve absorption efficiency due to localized surface plasmon resonance (LSPR), charge density oscillations at the surfaces of these core-shell composite nanoparticles. In this study, the effect of the geometry of TiO_2@Ag core-shell composite nanoparticles on their optical absorption properties was theoretically illustrated in the wavelength ranges between the visible and infrared light regions of electromagnetic radiation. These nanostructures were modeled by varying the TiO_2 core and Ag shell radii of the composite nanospheres and nanowires. The results indicate that varying the TiO_2 core radius and Ag shell thickness can be used to tune the absorption efficiency of these materials from the UV region to the visible or infrared regions of the electromagnetic spectrum. An increase in the absorption efficiency with greater core radii was observed. The absorption efficiency peaks of core-shell nanospheres or nanowires increased with the shell radius. Theoretical modeling based on these results suggest that this nanomaterial can be effectively utilized so that its optical absorption properties can be tuned. These properties could help to synthesize TiO_2@Ag core-shell composite NPs for use in environmental applications such as treating contaminated water and in novel future devices.

1. Introduction

Noble metal nanoparticles (NPs) such as gold (Au), copper (Cu), and silver (Ag) have been widely used for a variety of applications including photocatalysis systems [1-6] and solar cells [7,8]. They have been employed for thiram pesticide detection [9] and to enhance the performance of various devices. The absorbed and concentrated extra photon energy due to surface plasmonic resonance (SPR) arises with coherent collective oscillations of the conduction electrons of a metal and when the frequency of the incident light is in resonance with this plasma oscillation. If such oscillations occur in particles smaller than the wavelength of the incident light, the phenomenon known as localized surface plasmon resonance (LSPR) results. The resonance frequency is mainly determined by the particle dimensions (that is, the strength of the restoring force), the dielectric function of the particle, shape, polarization direction of the incident light, and the surrounding medium [10-16]. In Ag, Au, and Cu NPs, the LSPR can be excited by visible light. Their unique properties and combinations with other materials have therefore attracted much attention in the scientific community. One promising approach is the addition of noble metals to metal-oxide semiconducting nanomaterials of titanium dioxide (TiO_2), commonly called titania, to improve photocatalyst activity [1-6]. TiO_2 has proven to be a semiconductor material with widespread applications in the field of photocatalysis. It has been used for removing dangerous contaminants from drinking water, as well as degrading environmentally toxic dyes and organic pollutants [17]. However, its wide band gap energy (~3.2 eV) limits its potential application in the visible range of light irradiation [17]. The main component of the solar light reaching the Earth's surface is comprised of ~45% visible light, ~50% NIR with ~5% of ultraviolet light [18]. TiO_2 has a wide band gap making it sensitive only to ultraviolet (UV) light. Therefore, the photocatalytic activity of TiO_2 has insufficient light absorption when irradiated with sunlight due to the faster recombination of photogenerated charge carriers and the limited availability of ultraviolet (UV) light [17]. The photocatalytic mechanism is related to the electronic band structure theory of solids, which describes the electrical conductance of materials [19]. All materials have two energy bands, a lower band called a valence band and a higher conduction band. The difference between the highest energy level in the valence band and the lowest energy level in the conduction band is called the energy band gap. In this gap, no electron energy states can exist. Under irradiation with photons of equal or greater energy than the band gap, electrons in the valence band are excited into the conduction band, leaving holes in the valence band. In most cases, these pairs recombine and photon energy is lost to heat

DOI: 10.14456/jmmm.2020.35

dissipation. However, if the electrons or holes becomes trapped by a suitable scavenger or surface defect, the pair can be spatially separated allowing the photogenerated hole to reach the semiconductor surface and react to produce highly oxidizing radical species [17]. Several methods were proposed to make the photocatalyst reactive under visible light (λ >380 nm), such as decreasing the TiO_2 band gap energy. Among these methods, inclusion of noble metals to excite the LSPR can be used to improve the photocatalytic activity of TiO_2 by shifting the absorption band gap energy to the visible light region [2,18]. Therefore, in this work, we investigate optical improvement of TiO_2 by compounding it with a Ag nanoshell particle. The nanowire and spherical nanostructure of TiO_2@Ag core-shells, particles consisting of a TiO_2 core coated with a Ag nanoshell, were used as samples to improve the optical absorption of TiO_2. The optical properties of these structured particles can also be obtained using analytical solutions. The relationship between the spectral absorption characteristics, Ag shell thickness and the diameter of the TiO_2 core was elucidated using a computational analysis of the composite nanospheres and nanowires.

2. Experimental

Mie theory, which solves Maxwell's equations regarding the absorption and scattering of light from arbitrarily sized spherical and cylindrical particles, was employed herein to calculate optical properties. For single and coated spheres (Figures 1(a) and 1(b), respectively), a complete and detailed description of this method can be found in [20-22]. The absorption efficiency factor of a spherical core-shell nanoparticle can be expressed as an infinite series:

$$Q_{abs} = \frac{2\pi}{k^2}\sum_{n=1}^{\infty}(2n+1)\left[\mathrm{Re}\left(a_n + b_n\right) - |a_n|^2 - |b_n|^2\right] \quad (1)$$

where a_n and b_n are previously derived scattering coefficients [20-22], while $k = \frac{2\pi n_m}{\lambda}$ and n_m is the refractive index of the incident medium. Single and core-shell NWs are depicted in Figure 2(a) and 2(b), respectively. These particles were treated as infinitely long free-standing cylinders illuminated by a normal-incident plane wave. Solutions can be obtained by expanding the electric and magnetic field components of the incident and scattered light into infinite series of cylindrical vector harmonics. The incident electromagnetic fields are dependent on the polarization of the wave. One is the transverse electric (TE) or s-polarized light, where the electric field of the incoming wave is transverse to the axis of the cylinder. The other is the transverse magnetic (TM) or p-polarized light, where the magnetic field is transverse to the cylinder axis (see Figure 2). The absorption efficiency factors of incident TM waves as well as TE waves and unpolarized waves, respectively, are provided by [20,23-25].

$$Q_{abs,TM} = \frac{2}{x}\sum_{n=-\infty}^{\infty}\left[\mathrm{Re}\left(a_n\right) - |a_n|^2\right] \quad (2)$$

$$Q_{abs,TM} = \frac{2}{x}\sum_{n=-\infty}^{\infty}\left[\mathrm{Re}\left(b_n\right) - |b_n|^2\right] \quad (3)$$

Here, the geometric parameter is $x = \frac{2\pi}{\lambda} n_m R_c$, where n_m is the refractive index of the incident medium (water in this work) and R_c is the cylinder radius. Using Equation (2) and (3), the scattering efficiency due to the unpolarized waves is:

$$Q_{abs} = \frac{1}{2}\left(Q_{abs,TM} + Q_{abs,TE}\right) \quad (4)$$

For single nanowire of a pure material (Figure 2(a)), the coefficients a_n and b_n can be found in [20-22], whereas the coefficients a_n and b_n for a core-shell nanowire can be found in [23,26,27]. In this calculation, the wavelength dependent complex refractive indices for Ag were obtained from [28], and the corresponding data for TiO_2 was taken from [29]. The simulations were performed using water (n_m = 1.33) as the surrounding dielectric medium.

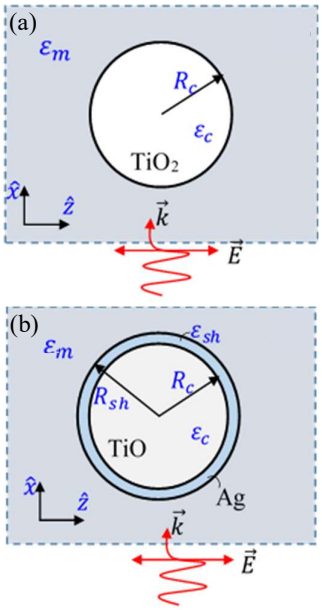

Figure 1. Schematic illustration of light scattering from (a) single pure TiO_2 and (b) TiO_2@Ag core-shell spherical nanoparticle structures simulated under plane-wave incidence along the x-axis.

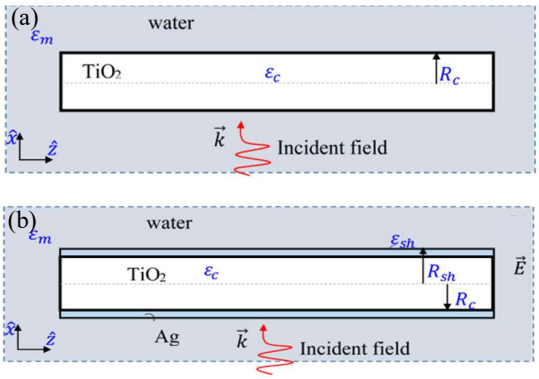

Figure 2. Schematic illustration of light scattering from infinite (a) single NWs and (b) core-shell NW structures simulated under a plane-wave incident perpendicular to its axis. The cylinder axis was elongated in the z axis.

3. Results and discussion

The calculated absorption spectra of isolated pure Ag and TiO_2 NPs in water are presented at wavelengths of 300-800 nm for electromagnetic (EM) waves, as shown in Figure 3. When nanoparticles are irradiated by incident light, free electrons collectively resonate. If the oscillation frequency identically matches the frequency of the irradiated light, the LSPR effect is responsible for the absorption peak. This is clearly seen in Figure 3(a) for the absorption spectra of pure, isolated spherical Ag nanoparticles. The dependence of the nanoparticle size on the optical absorption efficiency has been demonstrated. The results indicate that as the particle size increases, the maximum absorption or LSPR peak shifts to longer wavelengths. For example, an LSPR position 30 nm in diameter was found at ~388 nm. When the particle size was increased to 50 nm, 70 nm, and 100 nm, the LSPR position shifted to ~403 nm, ~423 nm, and ~468 nm, respectively. Additionally, as the diameter of the particles increased to greater than 30 nm, the efficiency spectra broadened. Moreover, a small quadrupolar shoulder was observed at higher energies (Figure 3(a)). This is because the subscript n of the Mie coefficients a_n and b_n in Equation (1) describes the angular momentum of atomic orbitals numbered as n =1,2,3,… for dipole, quadrupole, octopole, and higher order modes, respectively [10]. For a small diameter nanoparticle corresponding to $n = 1$, only the dipole mode is excited [10]. Consequently, only one dipole plasmon peak was observed (see Figure 3(a)). For larger particles, higher multipoles, especially the quadrupole term ($n = 2$), can occur and become important to the absorption properties [10]. Therefore, it can be seen that the dipole plasmon peak position became red-shifted, and there was a distinct quadrupole resonance peak at a lower wavelength (Figure 3(a)). Moreover, increasing the particle size resulted in significantly more electrons to scatter the radiated light. Eventually this dominated the spectrum and absorption became more broad and with less absorption intensity. Therefore, scattering dominates for large particles. In contrast, particle absorption dominates with small particles. Ag nanoparticles obviously exhibit strong optical absorption properties, that is, LSPR within the visible light region of EM radiation. Consequently, the induced EM field associated with the LSPR is considerably enhanced in the vicinity of nanoparticles [30]. Similar to pure Ag nanoparticles, Figure 3(b) shows the optical absorption efficiencies of TiO_2 nanoparticles in a photon wavelength range between 300 and 800 nm with varying particle sizes from 30 nm to 150 nm. The absorption spectrum at TiO_2 sizes at 30, 50, and 70 nm exhibits the typical optical absorption in the UV part of the spectrum for wavelengths shorter than 390 nm. Increasing the TiO_2 particle size led to absorption peaks at ~344 nm (3.60 eV) at a 100 nm diameter and ~354 nm (3.50 eV) and ~422 nm (2.93 eV) at a 150 nm diameter. As shown in Figure 3(b), the absorption intensity increases with the nanoparticle diameter. To extend the light absorption of TiO_2 into the visible region, thereby improving its performance in applications such as photocatalytic and sensitized solar cells (suitable band gap of ~3.27 eV), spherical nanoparticles were coated with Ag films as depicted in Figure 1b. The effects of the TiO_2 core radius and Ag shell thickness on the optical absorption spectra are illustrated in Figure 4. Figure 4(a) shows a shifting of the absorption peaks from a single pure TiO_2 nanoparticle and when the TiO_2 was coated with Ag film. By varying the Ag shell thickness in a range of 5-20 nm at a constant TiO_2 core diameter of 30 nm, two main peaks occurred in each sample. The TiO_2@Ag core-shell nanoparticle sample with a 5 nm thick shell had absorption peaks at ~336 nm (3.69 eV) and ~612 nm (2.02 eV). The 5 nm thick sample had absorption peaks at ~368 nm (3.37 eV) and ~456 nm (2.72 eV). All of the samples had similar absorption peaks in the visible region of the spectrum. As the shell thickness of the Ag film increased from 5 to 20 nm, the absorption peaks shifted toward to that of a pure single Ag particle (~388 nm, Figure 3(a)). It is clear that Ag nanoparticles can bring the absorption bands of TiO_2 nanoparticles from the UV light (see Figure 3(b)) to the visible light region. Similar to Figure 4(b), the absorption bands can be extended into the visible and infrared regions of the spectrum by varying the TiO_2 core radius from 5-50 nm at a fixed Ag shell thickness of 10 nm. The main absorption peaks of each sample gradually shifted from ~422 (2.94 eV) to ~508 (2.44 eV), ~590 (2.10 eV), ~666 (1.86 eV), and ~776 nm (1.59 eV) as the core radius increased from 5 to 15, 25, 35, and 50 nm, respectively. Two additional sets of peaks were observed in each sample, a spiculated peak from 330-470 nm and a small peak in the visible light region. It is clear that the introduction of the Ag film on the spherical nanoparticles of the TiO_2 surfaces resulted in TiO_2@Ag core-shell nanoparticles that extended the absorption edge into the visible light range. This was not found in the TiO_2 nanoparticles. More importantly, the decrease in the Ag shell thickness greatly enhanced the absorption intensity in the visible light range. For single pure Ag

and TiO_2 nanowires, the modelled sample in Figure 2 was used to simulate the optical absorption properties. Figure 5(a) shows the calculated non-polarized absorption spectra for cylindrical Ag nanowires of various dimensions in water. Absorption peaks were found at approximately 350-360 nm, which agrees with previously reported UV-vis absorption spectra data [30]. Meanwhile, the non-polarized absorption of the TiO_2 nanowire peaked in the UV region of the EM spectrum, which corresponds to previously reported UV-vis absorption spectral data [31]. However, there was a shift in the absorption peak to a higher wavelength in the visible region of the EM wave due to Ag film coating on the TiO_2 nanowire, as shown in Figure 6

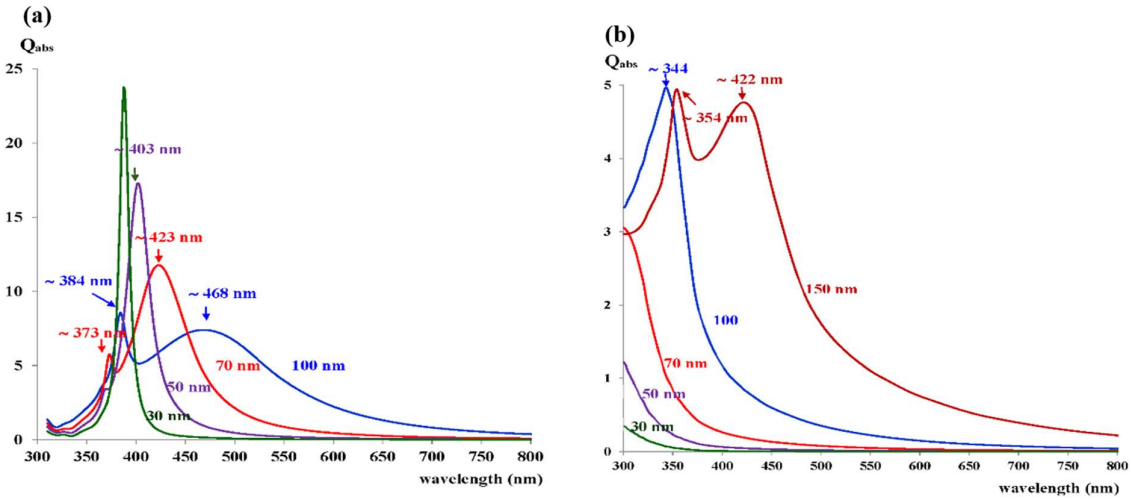

Figure 3. Calculated absorbance spectra of (a) pure Ag and (b) TiO_2 spherical NPs with diameters of 30, 50, 70, 100, and 150 nm embedded in water.

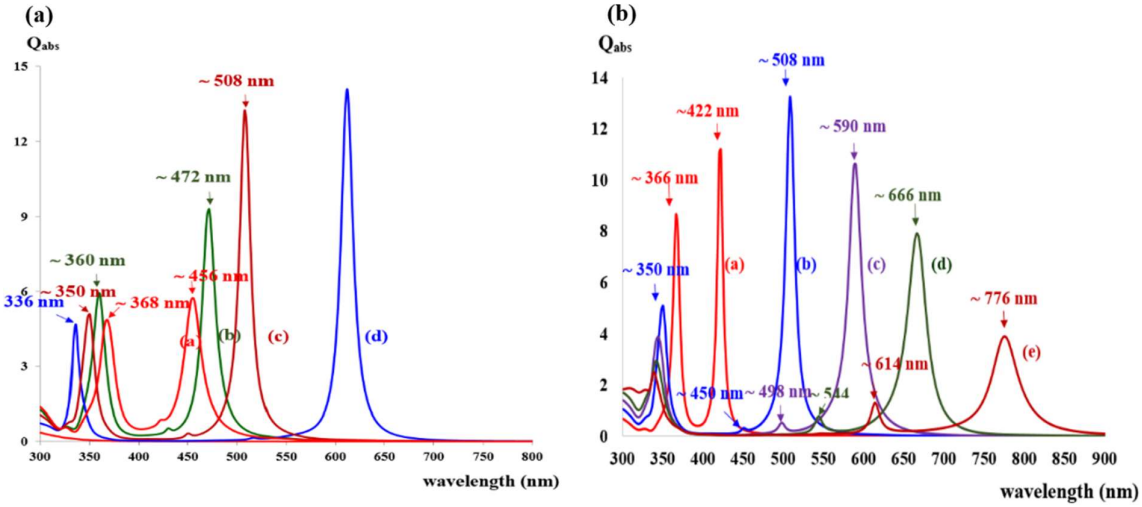

Figure 4. Calculated absorbance spectra of TiO_2@Ag core-shell NPs: (a) varying shell thicknesses to (1) 20 nm, (2) 15 nm, (3) 10 nm, and (4) 5 nm and (b) varying core radii to (1) 5 nm, (2) 15 nm, (3) 25 nm, (4) 35 nm, and (5) 50 nm.

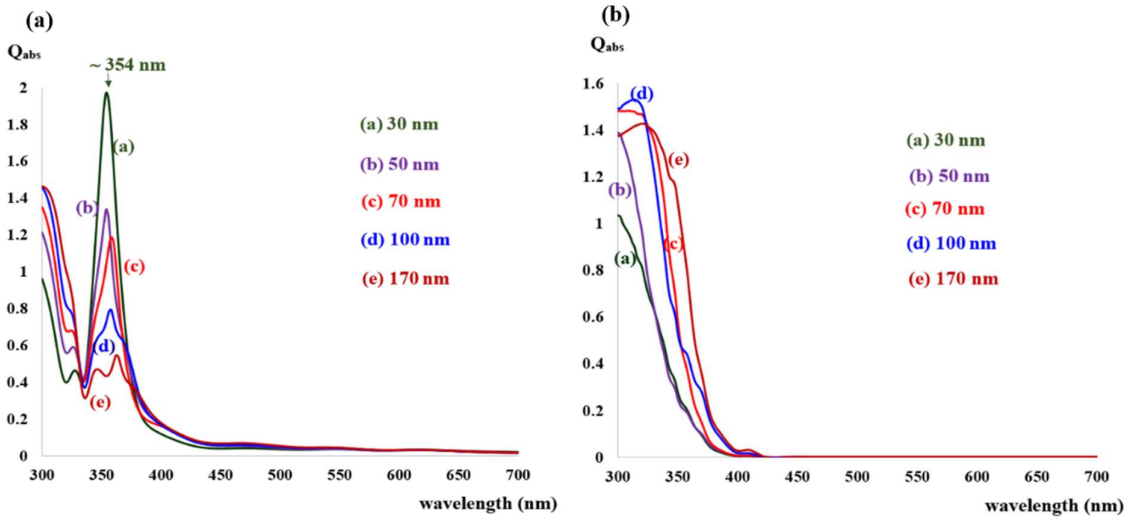

Figure 5. Calculated absorption spectra of single pure (a) Ag and (b) TiO_2 nanowires with various diameters as indicated by each line.

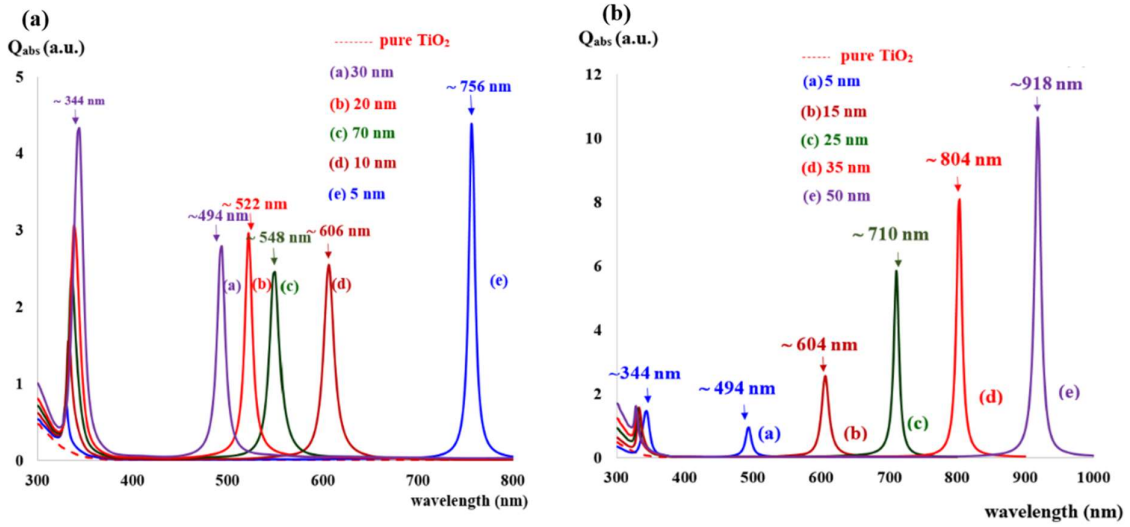

Figure 6. Calculated absorbance spectra of TiO_2@Ag core-shell nanowires: (a) varying Ag shell thicknesses to (1) 30 nm, (2) 20 nm, (3) 15 nm, (4) 10 nm, and (5) 5 nm and (b) varying core radii to (1) 5 nm, (2) 15 nm, (3) 25 nm, (4) 35 nm, and (5) 50 nm.

Figure 6 shows the calculated spectra of cylindrical TiO_2@Ag core-shell nanowires of various shell thicknesses of Ag film (see Figure 6(a)) and TiO_2 core radii (see Figure 6(a)) in water. TiO_2@Ag clearly has two additional peaks in each sample. The first set appears in a wavelength range of 300-400 nm and the other appears in the visible light region. Figure 6(a) shows the effect of the Ag shell thickness (in a range of 5-30 nm) on the absorption efficiency of composite nanowires under non-polarized excitation. The core radius of TiO_2 was fixed at 30 nm. A set of peaks in the visible region of the spectrum had resonances that were highly tunable, demonstrating a blue shift with increasing Ag shell thickness. It shifted from ~756 to ~606, ~548, ~522, and ~494 nm as the Ag thickness increased from 5 to 10, 15, 20, and 30 nm, respectively. Another set of peaks slightly shifted to longer wavelengths over the range of 330-350 nm. Figure 6(b) demonstrates the effects of varying the TiO_2 core radius from 5-50 nm (fixed at 10 nm Ag shell thickness) on the absorption efficiency of TiO_2@Ag core-shell nanowires. The maximum absorption of the spectrum under unpolarized excitation had a red shift when the TiO_2 core radius was increased from 5 to 50 nm. For example, at 35 and 50 nm TiO_2 core radii, respectively, the absorption peak shifted to ~804 and ~918 nm, to the

near infrared region of the EM radiation. At TiO_2 core radii of 5, 15, and 25 nm, the absorption peak shifted to ~494, ~604, and ~710 nm, i.e., to the visible region of the EM wave spectrum. For all of the calculated TiO_2@Ag core-shell nanostructures, when varying the TiO_2 core and Ag shell thicknesses, strong optical absorption resonance can be placed virtually anywhere across the visible or infrared regions of the EM spectrum. The surface plasmon absorption peak position is extremely sensitive to particle size and shape, as well as the properties of the surrounding medium and the polarization direction of incident light [10,23]. In experimental work, for most of the synthesized materials, it was found that the direction of each particle's axis in the sample was random [24,25]. Consequently, they can be characterized using the light coming from either the x or z directions, as shown in Figure 2. The surface plasmon absorption peak position should be slightly shifted from that obtained in the current work. Variation of the electron population, treated as a free electron gas, on the noble metal nanoparticles and the plasmon mode coupling theories [32-35] are two commonly reported explanations for the shift in the plasmonic peaks. Based on variation in the electron population due to the resonance frequency, ω_p is defined by

$$\omega_p = \left(\frac{Ne^2}{m * \varepsilon_0} \right)^{0.5}$$

where ε_0 is the vacuum permittivity, $m*$ is the electron's effective mass, e is the electronic charge, and N is the bulk charge density. Therefore, the shift in the LSPR peak to longer wavelengths due to the thicker Ag shell should involve a higher number of free electrons. In plasmon mode coupling theory, two distinct plasmon modes of an outer and an inner shell surface cavity mode of the Ag shell are produced, causing the LSPR to split into anti-bonding and symmetric plasmons. Anti-bonding coupling results in a lower wavelength-shifted mode, whereas bonding coupling corresponds to a higher wavelength-shift of the LSPR peak. The coupling energy is proportional to a geometric parameter defined as the ratio between the inner and outer radii of the metallic shell. The result is that the metallic shell thickness is associated with the strength of the plasmon interaction. This phenomenon, therefore, determines the LSPR position.

Environmental applications of TiO_2 nanoparticles, such as antibacterials based on photo-induced decomposition reactions, [1-5] involve modification of TiO_2 sensitivity to visible light. TiO_2@Ag core-shell structured nanoparticles can serve as new materials capable of uniquely controlled optical absorption properties in the visible and infrared spectral regions. Based on the results of this work, TiO_2@Ag core-shell structured nanoparticles can be developed to help understand the scientific basis of this behavior and engineer fundamental optical properties along with potential novel applications, which may not be possible with pure TiO_2.

4. Conclusions

In summary, the optical absorption properties of TiO_2@Ag core-shell structured nanoparticles are presented based on analytical calculations using electrostatic approximations. Compared to pure Ag and TiO_2 nanoparticles, the optical properties of TiO_2@Ag core-shell nanospheres and nanowires can be controlled through variation of the core radius and shell thickness. Consequently, the optical absorption peak position of these nanoparticles can be tuned from the UV region to the visible or infrared regions of the EM radiation spectrum in a water medium. More importantly, in both TiO_2@Ag core-shell nanospheres and nanowires, the absorption peaks were shifted to longer wavelengths compared to pure TiO_2 nanoparticles. This red shift became more pronounced as the TiO_2 core radius was increased. Conversely, the absorption peak blue-shifted when the thickness of the Ag shell increased. Therefore, the optical absorption properties of TiO_2 nanoparticles can be modified so that they are sensitive to visible light. Theoretical modeling based on optical absorption properties suggests that the optical absorption of this nanomaterial can be effectively tuned across the visible and infrared regions of the EM wave spectrum. These results can help to synthesize TiO_2@Ag core-shell composite NPs for use in environmental applications and new devices in the future.

5. Acknowledgements

The Integrated Research Group financially supported this work for Energy and Environment (IRGEE), Khon Kaen University, Nong Khai Campus, Nong Khai. The authors acknowledge the facilities and support of the Faculty of Interdisciplinary Studies, Nong Khai Campus, Khon Kaen University.

References

[1] P. V. Kamat, Photophysical, "Photochemical and Photocatalytic Aspects of Metal Nanoparticles", *Journal of Physical Chemistry B,* vol. 106, pp. 7729-7744, 2002.

[2] V. Subramanian, E. E. Wolf and P. V. Kamat, "Catalysis with TiO_2/gold nanocomposites. Effect of metal particle size on the Fermi level equilibration", *Journal of the American Chemical Society,* vol. 126, pp. 4943-4950, 2004.

[3] J. Goebl, J.B. Joo, M. Dahl and Y. Yin, "Synthesis of Tailored Au@TiO_2 Core-Shell", *Catalysis Today,* vol. 225, pp. 90-95, 2014.

[4] S. Sreeja, and K. V. Shetti, "Photocatalytic water disinfection under solar irradiation by Ag@TiO_2 core-shell structured nanoparticles", *Solar Energy*, vol. 157, pp. 236-243, 2017.

[5] J. Prakash, S. Sun, H. C. Swart and R. K. Gupta, "Noble metals-TiO_2 nanocomposites", *Applied Materials Today*, vol. 11, pp. 82-135

[6] J. Thapoung, K. Tasurin, N. Traiphol, and N. Pangpaiboon, "The effects of concentrations of ZnO nanoparticles on dewetting suppression of PS thin films", *Journal of Metals, Materials and Minerals,* vol. 28, pp. 89-93, 2018.

[7] D. M. Schaadt, B. Feng and E. T. Yu, "Enhanced semiconductor optical absorption via surface plasmon excitation in metal nanoparticles", *Applied Physics Letters,* vol. 86, pp. 063106-1–063106-3, 2005.

[8] Y. Yang, J. Wu and J. Li, "Correlation of the plasmon-enhanced photoconductance and photovoltaic properties of core-shell Au@TiO_2 network", *Applied Physics Letters,* vol. 109, pp. 091604, 2016.

[9] P. Guo, D. Sikdar, X. Huang, K.J. Si, W. Xiong, S. Gong and L.W. Yap, "Plasmonic core-shell nanoparticles for SERS detection of the pesticide thiram: size- and shape-dependent Raman enhancement", *Nanoscale,* vol. 7, pp. 2862-2868, 2015.

[10] K. L. Kelly, E. Coronado, E. L. Zhao and G.C. Schatz, "The Optical properties of metal nanoparticles: The influence of size, shape, and dielectric environment", *Journal of Physical Chemistry B,* vol. 107, pp. 668-677, 2003.

[11] K. S. Lee and M. A. El-Sayed," Dependence of the enhanced optical scattering efficiency relative to that of absorption for gold metal nanorods on aspect ratio, size, end-cap shape, and medium refractive index", *Journal of Physical Chemistry B,* vol. 109, pp. 20331-20338, 2005.

[12] T. Dasri and S. Sompech,"Simulation of absorption spectra of metal nanoparticles embedded in organic media", *Integrated Ferroelectrics,* vol. 165, pp. 176-184, 2015.

[13] T. Dasri, "Theoretical calculation of plasmonic enhancement of silver nanosphere, nanocube, and nanorod embedded in organic solar cells", *Integrated Ferroelectrics,* vol. 175, pp. 176-185, 2016.

[14] A. Chingsungnoen and T. Dasri, "Optical properties of single gold nanoparticle embedded in organic medium", *Materials Today: Proceedings,* vol. 5, pp. 11027-11034, 2018.

[15] T. Dasri and A. Chingsungnoen, "Surface plasmon resonance enhanced light absorption and wavelength tuneable in gold-coated iron oxide spherical nanoparticle", *Journal of Magnetism and Magnetic Materials*, vol. 456, pp. 368–371, 2018.

[16] S. Sompech, S. Thaomola, A. Chingsungnoen and T. Dasri, "Theoretical calculation of optical absorption property of Cu@Ag core–shell composite nanoparticle", *Materials Research Express,* vol. 6, pp. 026201, 2019.

[17] S. Malato, P. Fernandez-Ibanez, M. I. Maldonado, J. Blanco and W. Gernjak, "Decontamination and disinfection of water by solar photocatalysis: Recent overview and trends", *Catalysis Today*, 2009, 147: 1-59

[18] Y. Jiaguo, D. Gaopeng and H. Baibiao, "Fabrication and characterization of visible-light-driven plasmonic photocatalyst Ag/AgCl/TiO_2 Nanotube Arrays", *Journal of Physical of Chemistry C*, 2009, vol. 113, pp. 16394–16401, 2009.

[19] R. M. N. Yerga, M. C. A. Galvan, F. del Valle, J. A. V. de la Mano and J. L. G. Fierro, "Water splitting on semiconductor catalysts under visible-light irradiation", *ChemSusChem*, vol. 2, pp. 471-485, 2009.

[20] C. F. Bohrem and D. R. Huffman, "Absorption and scattering of light by small particles." New York: Wiley-Interscience, 1983.

[21] J. L. W. Li, Z. C. Li, Y. She, S. Zouhdi, J. R. Mosig, S. Zouhdi, I. R. Mosig and O. J. F. Martin, "Solution to light scattering by spherical nanoshells", *IEEE Transactions Nanotechnology*, vol. 8, pp. 617–626, 2009.

[22] P. Chaiyachate, A. Chingsungnoen, T. Dasri, "Theoretical calculation of the optical properties of dielectric material @ noble metal core-shell composite nanoparticles", *Indian Journal of Science and Technology,* vol. 10, pp. 1-8, 2017.

[23] L. Cao, P. Fan, E. S. Barnard, A. M. Brown and M. L. Brongersma, "Tuning the color of silicon nanostructures", *Nano Letters,* vol. 10, pp. 2649-2654, 2010.

[24] G. Bronstrup, N. Jahr, C. Leiterer, A. Csaki, W. Fritzsche and S. Christiansen, "Optical properties of individual silicon nanowires for photonic devices", *ACS Nano*, vol. 4, pp. 7113-7122, 2010.

[25] J. F. Zimmerman, G. F. Murray and B. Tian, "Optical determination of silicon nanowire diameters for intracellular applications", *Journal of Physical Chemistry C*, vol. 119, pp. 29105-29115, 2015.

[26] P. Y. Chen, J. Soric and A. Alù, "Invisibility and cloaking based on scattering cancellation", *Advanced Materials*, vol. 24, pp. OP281-OP304, 2012.

[27] K. H. Kim and Y. S. No, "Subwavelength core/shell cylindrical nanostructures for novel plasmonic and metamaterial devices", *Nano Convergence,* vol. 4, pp. 1-13, 2017.

[28] P. B. Johnson and R. W. Christy, "Optical constants of the noble metals", *Physical Review B*, vol. 6, pp. 4370-4379, 1972.

[29] L. Skowronski, A. A. Wachowiak and A. Grabowski, "Characterization of optical and microstructural properties of semitransparent TiO_2/Ti/glass interference decorative coatings", *Applied Surface Science,* vol. 388, pp. 731-740, 2016.

[30] B. Bari, J. Lee, T. Jang, P. Won, S. H. Ko, K. Alamgir, M. Arshad and L. J. Guo, "Simple hydrothermal synthesis of very-long and thin silver nanowires and their application in high quality transparent electrodes", *Journal of Materials Chemistry A,* vol. 4, pp. 11365-11371, 2016.

[31] C. Peng, W. Wang, W. Zhang, Y. Liang and L. Zhuo, "Surface plasmon-driven photoelectrochemical water splitting of TiO_2 nanowires decorated with Ag nanoparticles under visible light illumination", *Applied Surface Science,* vol. 420, pp. 286-295, 2017.

[32] E. Prodan and P. Nordlander," Structural Tunability of the Plasmon Resonances in Metallic Nanoshells", *Nano Letters*, vol. 3, pp. 543-547, 2003.

[33] E. Prodan and P. Nordlander, "Plasmon hybridization in spherical nanoparticles", Journal *of Chemical Physics*, vol. 120, pp. 5444-5454, 2004.

[34] M. D. Turner, M. M. Hossain, and M. Gu, "The effects of retardation on plasmon hybridization within metallic nanostructures", *New Journal of Physics*, vol. 12, pp. 083062, 2010.

[35] A. Aubry, D. Y. Lei, S. Maier and J. B. Pendry, "Plasmonic hybridization between nanowires and a metallic surface: A transformation optics approach", *ACS Nano*, vol. 5, pp. 3293-3308, 2011.2018.